



Natural convection heat transfer between bodies and their enclosures  
by Robert O'Neil Warrington, Jr

A thesis submitted in partial fulfillment of the requirements for the degree of DOCTOR OF  
PHILOSOPHY in Mechanical Engineering  
Montana State University  
© Copyright by Robert O'Neil Warrington, Jr (1975)

**Abstract:**

Natural convection heat transfer between concentrically located isothermal spherical, cylindrical, and cubical inner bodies and their isothermal cubical enclosure (with air, water, 20 cs silicone oil, and glycerin in the test space) was experimentally investigated. Comparisons were made with the existing data for these same inner bodies and a spherical enclosure. In addition, temperature distributions and flow visualization data were obtained for most of these geometries.

Temperature profiles were taken at five angular positions ( $\theta = 0^\circ, 34^\circ, 80^\circ, 120^\circ, 160^\circ$ ) and in two vertical planes. The form of the dimensionless temperature profiles were practically invariant with changes in inner body, outer body, and vertical plane. An increase in the Prandtl number increased the magnitude of the dimensionless temperature and also increased the magnitude and extent of the temperature inversions. The ordering of the temperature profiles changed with increased  $G/Ri$  and  $\Delta T$ .

Comparisons made between the spherical and cubical enclosure, for the same inner body types, showed that the cubical enclosure resulted in a larger Nusselt number for a given Rayleigh number and inner body size. Heat transfer data taken with a non-isothermal inner body showed that the isothermality conditions on the inner body could be relaxed. The independent correlating parameters used in this study were the Prandtl number, Rayleigh number (based on both hypothetical gap width,  $L$ , and boundary layer length,  $b$ ), the modified Rayleigh number (based on the same length parameters), and the gap to radius ratio,  $L/R_j$ . The ranges of these parameters were:  $0.706 < Pr < 13847$ ,  $1.8 \cdot 10^3 < Ra_l < 1.1 \cdot 10^9$ ,  $4.6 \cdot 10^5 < Ra_b < 4.0 \cdot 10^{10}$ ,  $165 < Ra_L < 2 \cdot 10^9$ ,  $2.9 \cdot 10^6 < Ra_b < 3.0 \cdot 10^{10}$ , and  $0.07 < L/R_i < 2.15$ .

The best overall empirical equation (for both the spherical and cubical enclosure data) utilizing a single independent correlating parameter was  $Nu_b = 0.585 Ra_b^{0.236}$  for the range of  $Pr$  and  $Ray$  given above. It was also determined that the ratio  $q_{conv}/q_{cond}$  correlated the data better than the Nusselt number for small  $L/R_i$ . It is the author's opinion that the above equation could be used, with a high degree of confidence, to predict the heat transfer between arbitrarily shaped inner and outer bodies. This statement is a direct consequence of the fact that changes in the inner and outer body geometries had only minor influence on the overall heat transfer.

NATURAL CONVECTION HEAT TRANSFER BETWEEN  
BODIES AND THEIR ENCLOSURES

by

ROBERT O'NEIL WARRINGTON, JR.

A thesis submitted in partial fulfillment  
of the requirements for the degree

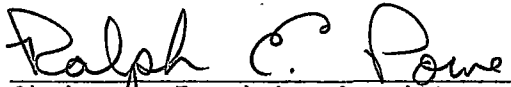
of


DOCTOR OF PHILOSOPHY

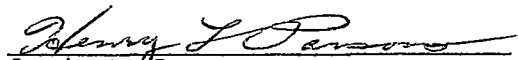
in

Mechanical Engineering

Approved:

  
Chairman, Examining Committee

  
Head, Major Department

  
Graduate Dean

MONTANA STATE UNIVERSITY  
Bozeman, Montana

December, 1975

## ACKNOWLEDGMENT

The author would like to express his appreciation to all those who provided assistance during the course of this investigation. The writer is especially thankful to Dr. R. E. Powe for his example, advice, and guidance. The author is also very appreciative of the help from the other members of his committee; Dr. R. L. Mussulman, Dr. J. A. Scanlan, Professor R. C. Challender, and Dr. M. S. Henry. Thanks also go to Gordon Williamson who constructed the apparatus. The author is especially indebted to his wife, Anne, who was an invaluable asset during the completion of this work. The writer would also like to thank Bobby and Danny, his children, who have put up with (or without) their father during the final stages of this work.

The work in this dissertation was supported by the National Science Foundation under Grant Number GK-31908, the Atomic Energy Commission under AEC Contract Number AT(45-1)-2214, and by the Mechanical Engineering Department at Montana State University.

## TABLE OF CONTENTS

| <u>Chapter</u>   | <u>Page</u> |
|--|-------------|
| VITA . . . . .   | ii          |
| ACKNOWLEDGMENT . . . . .   | iii         |
| LIST OF TABLES . . . . .   | v           |
| LIST OF FIGURES. . . . .   | vi          |
| ABSTRACT . . . . .   | xi          |
| NOMENCLATURE . . . . .   | xii         |
| I. INTRODUCTION . . . . .  | 1           |
| II. LITERATURE REVIEW . . . . .  | 4           |
| III. EXPERIMENTAL APPARATUS AND PROCEDURE. . . . .                               | 19          |
| IV. DISCUSSION OF HEAT TRANSFER RESULTS' . . . . .                               | 35          |
| V. DISCUSSION OF TEMPERATURE PROFILE AND FLOW VISUALIZATION<br>RESULTS . . . . . | 95          |
| VI. CONCLUSION. . . . .  | 129         |
| APPENDIX I . . . . .   | 136         |
| APPENDIX II. . . . .   | 149         |
| APPENDIX III . . . . .   | 182         |
| BIBLIOGRAPHY . . . . .   | 199         |

## LIST OF TABLES

| <u>Table</u>   | <u>Page</u> |
|--|-------------|
| 3.1 Geometries used with Spherical Outer Body . . . . .                                | 26          |
| 3.2 Geometries used with Cubical Outer Body . . . . .                                  | 27          |
| 4.1 Range of the Independent Correlating Parameters . . . . .                          | 37          |
| 4.2 Correlation Equations for the Cube-Sphere Geometry. . . . .                        | 47          |
| 4.3 Correlation Equations for the Sphere-Cube Geometry. . . . .                        | 54          |
| 4.4 Correlation Equations for the Cylinder-Cube Geometry. . . . .                      | 64          |
| 4.5 Correlation Equations for the Cube-Cube Geometry. . . . .                          | 74          |
| 4.6 Correlation for each Inner Body Type. . . . .                                      | 91          |
| 4.7 Correlation for each Outer Body Type. . . . .                                      | 92          |
| 4.8 Correlation Equations for All the Enclosure Data. / . . . .                        | 93          |
| A2.1 Cubic Spline Curvefits of Conduction Solutions. . . . .                           | 167         |
| A2.2 Cubic Spline Curvefits of Conduction Solutions<br>Cylindrical Inner Body. . . . . | 168         |

## LIST OF FIGURES

| <u>Figure</u>  | <u>Page</u> |
|--|-------------|
| 3.1 Heat Transfer Apparatus. . . . .   | 20          |
| 3.2 Schematic of Heat Transfer Apparatus with Supporting<br>Instrumentation. . . . .                                     | 21          |
| 3.3 Spherical, Cylindrical and Cubical Inner Bodies. . . . .   | 23          |
| 3.4 Heat Loss by Stem Conduction and Gap Radiation Data. . . . .   | 32          |
| 4.1 Heat Transfer Data for the Cube-Sphere, Sphere-Cube,<br>Cylinder-Cube and Cube-Cube Geometries . . . . .             | 39          |
| 4.2 Heat Transfer Correlations for All of the Cube-Cube Data<br>and Each Individual Inner Body . . . . .                 | 41          |
| 4.3 Various Correlation Schemes for the Cube-Sphere Data and<br>Glycerin . . . . .                                       | 42          |
| 4.4 Heat Transfer Correlations for All the Cube-Sphere Data<br>and Each Individual Fluid. . . . .                        | 45          |
| 4.5 Heat Transfer Correlation for All of the Cube-Sphere Data. . . . .   | 46          |
| 4.6 Effect of Fluid Viscosity on the Sphere-Cube Data. . . . .   | 49          |
| 4.7 Heat Transfer Correlations for All of the Sphere-Cube Data<br>and Each Individual Inner Body . . . . .               | 51          |
| 4.8 Heat Transfer Correlations for All of the Sphere-Cube Data<br>and Each Individual Fluid. . . . .                     | 52          |
| 4.9 Overall Heat Transfer Correlation for the Sphere-Cube<br>Geometry . . . . .  | 53          |
| 4.10 Comparison of the Spherical Inner Bodies with the Cubical<br>and Spherical Enclosures for the 20 cs Fluid . . . . . | 57          |
| 4.11 Heat Transfer Data for All the Cylinders and the 20 cs<br>Fluid. . . . .  | 58          |
| 4.12 Heat Transfer Correlations for All of the Cylinder-Cube<br>Data and Each Individual Inner Body. . . . .             | 59          |

| <u>Figure</u>  | <u>Page</u> |
|--|-------------|
| 4.13 Heat Transfer Correlations for All of the Cylinder-Cube Data and Each Individual Fluid. . . . .   | 61          |
| 4.14 Overall Heat Transfer Correlation for the Cylinder-Cube Geometry. . . . .   | 62          |
| 4.15 Comparison of the Cylindrical Inner Bodies with the Spherical and Cubical Outer Bodies for the 20cs Fluid . . .                             | 63          |
| 4.16 Comparison of the Heat Transfer Data for the Rotated Cube with the Data for the Cube in its Standard Position . . . .                       | 67          |
| 4.17 All of the Glycerin Data for the Cubical Inner Bodies. . .  | 68          |
| 4.18 Heat Transfer Correlations for All of the Cube-Cube Data and Each Individual Body. . . . .  | 69          |
| 4.19 Heat Transfer Correlations for All of the Cube-Cube Data and Each Individual Fluid . . . . .  | 70          |
| 4.20 Overall Heat Transfer Correlation for the Cube-Cube Geometry. . . . .   | 71          |
| 4.21 Comparison of the Cubical Inner Bodies with Spherical and Cubical Outer Bodies and 20 cs Fluid. . . . .                                     | 73          |
| 4.22 Comparison of the Isothermal Inner Body Data with the Non-Isothermal Inner Body Data for the 4.0 and 6.4 inch Cubical Inner Bodies. . . . . | 77          |
| 4.23 All of the Non-Isothermal Inner Body Heat Transfer Data . .   | 79          |
| 4.24 Heat Transfer Correlations for All of the Spherical Enclosure Data and Each Inner Body Type . . . . .                                       | 81          |
| 4.25 Heat Transfer Correlations for All of the Cubical Enclosure Data and Each Inner Body Type . . . . .   | 82          |
| 4.26 Heat Transfer Correlations for All of the Heat Transfer Data and Each Enclosure Type. . . . .   | 85          |
| 4.27 Heat Transfer Correlations for All of the Enclosure Data and Each Individual Fluid. . . . .   | 86          |

| <u>Figure</u>   | <u>Page</u> |
|---|-------------|
| 4.28 Heat Transfer Correlation for All of the Heat Transfer Data and Each Enclosure Type . . . . .  | 87          |
| 5.1 Variation of Temperature Profile with $\Delta T$ , 7.0 inch Sphere ( $G/r_i = 0.50$ ) and Air, Perpendicular Plane . . . . .                                    | 97          |
| 5.2 Variation of Temperature Profile with $\Delta T$ , 7.0 inch Sphere ( $G/r_i = 0.50$ ) and Air, Diagonal Plane . . . . .   | 98          |
| 5.3 Flow Patterns for the 4.5 x 6.35 inch Cylinder and Air . . . . .  | 100         |
| 5.4 Comparison of the Perpendicular and Diagonal Planes, 7 x 8.1 inch Cylinder ( $G/r_i = .34$ ) and Glycerin, $Pr = 4104$ and $\Delta T = 47.65^\circ F$ . . . . . | 102         |
| 5.5 Prandtl Number Effect on the Temperature Profiles for the 4.5 inch Sphere ( $G/r_i = 1.33$ ), Perpendicular Plane . . . . .                                     | 103         |
| 5.6 Prandtl Number Effect on the Temperature Profile for the 4.5 x 6.35 inch Cylinder ( $G/r_i = 0.92$ ), Perpendicular Plane . . . . .                             | 104         |
| 5.7 Prandtl Number Effect on the Temperature Profile for the 5.0 inch Cube ( $G/r_i = 1.10$ ), Perpendicular Plane. . . . .   | 105         |
| 5.8 Flow Pattern for the 4.5 x 6.35 inch Cylinder and 20cs Fluid, $\Delta T = 115.6^\circ F$ . . . . .  | 107         |
| 5.9 Temperature Profiles for the 9.0 inch Sphere ( $G/r_i = 0.17$ ) and 20 cs Fluid; $\Delta T = 56^\circ F$ , $Pr = 231$ , Perpendicular Plane. . . . .            | 109         |
| 5.10 Temperature Profiles for the 7 x 8.9 inch Cylinder ( $G/r_i = 0.23$ ) and Air; $\Delta T = 29^\circ F$ , $Pr = .712$ , Perpendicular Plane . . . . .           | 110         |
| 5.11 Temperature Profiles for the 7 x 8.1 inch Cylinder ( $G/r_i = 0.34$ ) and Air, $\Delta T = 31^\circ F$ , $Pr = .710$ , Perpendicular Plane . . . . .           | 111         |
| 5.12 Flow Pattern for the 7 x 8.9 inch Cylinder and 20cs Fluid, $\Delta T = 33^\circ F$ . . . . .   | 112         |



| <u>Figure</u>  | <u>Page</u> |
|--|-------------|
| 5.13 Variation of the Temperature Profiles with $\Delta T$ , 7.0 inch<br>( $G/r_i = 0.50$ ) Sphere and 20 cs Fluid, Perpendicular Plane .          | 113         |
| 5.14 Temperature Profiles for All of the Cubical Inner Bodies<br>and 20 cs, Perpendicular Plane . . . . .  | 115         |
| 5.15 Flow Patterns for the 4.0 inch Cubical Inner Body<br>and Air . . . . .  | 116         |
| 5.16 Comparison of the Temperature Profiles for the 6.5 inch Cube<br>in its Standard and Rotated Positions (20 cs) . . . . .                       | 117         |
| 5.17 Comparison of the Temperature Profiles for the 6.4 inch<br>Cube in its Standard and Rotated Positions (20 cs) . . . . .                       | 118         |
| 5.18 Comparison of the Temperature Profiles for the Different<br>Inner Body Types and Air, Perpendicular Plane . . . . .                           | 120         |
| 5.19 Comparison of the Temperature Profiles for the Different<br>Inner Body Types and Glycerin, Perpendicular Plane . . . . .                      | 121         |
| 5.20 Flow Pattern of the 4.5 x 8.9 inch Cylinder and Air,<br>$\Delta T = 15^\circ F$ . . . . .   | 123         |
| 5.21 Comparison of the Temperature Profiles for the Sphere-<br>Sphere [45] and Sphere-Cube Geometries; Air,<br>Perpendicular Plane . . . . .       | 124         |
| 5.22 Comparison of the Temperature Profiles for the Sphere-<br>Sphere [15] and Sphere-Cube Geometries; 20cs,<br>Perpendicular Plane . . . . .      | 125         |
| 5.23 Comparison of the Temperature Profiles for the Cylinder-<br>Sphere [27] and Cylinder-Cube Geometries; 20 cs,<br>Perpendicular Plane . . . . . | 126         |
| 5.24 Comparison of the Temperature Profiles for the Cube-<br>Sphere and Cube-Cube Geometries; Glycerin,<br>Perpendicular Plane . . . . .           | 127         |

| <u>Figure</u>   | <u>Page</u> |
|---|-------------|
| 5.25 Comparison of the Temperature Profiles for the Cube-Sphere [27] and Cube-Cube Geometries, Air, Perpendicular Plane . . . . . | 128         |
| A2.1 Cube-Sphere Geometry . . . . .   | 150         |
| A2.2 Cube-Sphere Geometry in Two Dimensions . . . . .   | 157         |
| A2.3 Conduction Solution for the Cube-Sphere Geometry . . . . .   | 159         |
| A2.4 Sphere-Cube Geometry in Two Dimensions . . . . .   | 160         |
| A2.5 Conduction Solution for the Sphere-Cube Geometry . . . . .   | 162         |
| A2.6 Cylinder-Cube Geometry in Two Dimensions . . . . .   | 163         |
| A2.7 Conduction Solution for the Cylinder-Cube Geometry . . . . .   | 164         |
| A2.8 Conduction Solution for the Cube-Cube Geometry . . . . .   | 165         |

## ABSTRACT

Natural convection heat transfer between concentrically located isothermal spherical, cylindrical, and cubical inner bodies and their isothermal cubical enclosure (with air, water, 20 cs silicone oil, and glycerin in the test space) was experimentally investigated. Comparisons were made with the existing data for these same inner bodies and a spherical enclosure. In addition, temperature distributions and flow visualization data were obtained for most of these geometries.

Temperature profiles were taken at five angular positions ( $\theta = 0^\circ, 34^\circ, 80^\circ, 120^\circ, 160^\circ$ ) and in two vertical planes. The form of the dimensionless temperature profiles were practically invariant with changes in inner body, outer body, and vertical plane. An increase in the Prandtl number increased the magnitude of the dimensionless temperature and also increased the magnitude and extent of the temperature inversions. The ordering of the temperature profiles changed with increased  $G/R_i$  and  $\Delta T$ .

Comparisons made between the spherical and cubical enclosure, for the same inner body types, showed that the cubical enclosure resulted in a larger Nusselt number for a given Rayleigh number and inner body size. Heat transfer data taken with a non-isothermal inner body showed that the isothermality conditions on the inner body could be relaxed. The independent correlating parameters used in this study were the Prandtl number, Rayleigh number (based on both hypothetical gap width,  $L$ , and boundary layer length,  $b$ ), the modified Rayleigh number (based on the same length parameters), and the gap to radius ratio,  $L/R_i$ . The ranges of these parameters were:

$$0.706 < Pr < 13847, 1.8 \cdot 10^3 < Ra_L < 1.1 \cdot 10^9,$$

$$4.6 \cdot 10^5 < Ra_b < 4.0 \cdot 10^{10}, 165 < Ra_L^* < 2 \cdot 10^9,$$

$$2.9 \cdot 10^6 < Ra_b^* < 3.0 \cdot 10^{10}, \text{ and } 0.07 < L/R_i < 2.15.$$

The best overall empirical equation (for both the spherical and cubical enclosure data) utilizing a single independent correlating parameter was

$$Nu_b = 0.585 Ra_b^{*0.236}$$

for the range of  $Pr$  and  $Ra_b^*$  given above. It was also determined that the ratio  $q_{conv}/q_{cond}$  correlated the data better than the Nusselt number for small  $L/R_i$ . It is the author's opinion that the above equation could be used, with a high degree of confidence, to predict the heat transfer between arbitrarily shaped inner and outer bodies. This statement is a direct consequence of the fact that changes in the inner and outer body geometries had only minor influence on the overall heat transfer.

## NOMENCLATURE

| <u>Symbol</u> | <u>Description</u>   |
|---------------|--|
| a             | Any characteristic length  |
| $A_{1-7}$     | Defined by equations (A2.15)-(A2.21)   |
| $A_{cc}$      | Surface area of the copper-constantan thermocouples                          |
| $A_{htl}$     | Surface area of the heater tape leads  |
| $A_i$         | Surface area of the inner body   |
| $A_o$         | Surface area of the outer body   |
| $A_s$         | Surface area of the support stem   |
| b             | Distance traveled by the boundary layer on the inner body                    |
| $C, C_{1-4}$  | Empirically determined constants   |
| $c_p$         | Specific heat at constant pressure   |
| D             | Sphere diameter  |
| $D_i$         | Inner body diameter  |
| $D_o$         | Outer body diameter  |
| e             | Eccentricity, positive upward  |
| f             | Denotes function   |
| g             | Acceleration of gravity, 32.174 ft/sec <sup>2</sup>                          |
| G             | Defined by $\frac{(\text{outer cube length} - \text{inner body length})}{2}$ |

| <u>Symbol</u> | <u>Description</u>   |
|---------------|--|
| $Gr_a$        | Grashof number, $\rho^2 g \beta (T_i - T_o) a^3 / \mu^2$ , where $a$ is any characteristic dimension |
| $\bar{h}$     | Average heat transfer coefficient $\bar{h} = q_{conv} / A_i \Delta T$                                |
| $H$           | Total cylinder height  |
| $k$           | Thermal conductivity   |
| $k_{cc}$      | Thermal conductivity of the copper-constantan thermocouples  |
| $k_{eff}$     | Effective thermal conductivity   |
| $k_{htl}$     | Thermal conductivity of the heater tape leads  |
| $k_s$         | Thermal conductivity of the support stem   |
| $L$           | Gap width or hypothetical gap width, $R_o - R_i$   |
| $l$           | Length of straight cylindrical section   |
| $\Delta l$    | Change in length   |
| $n$           | Order of iteration   |
| $Nu_a$        | Nusselt number, $\bar{h} a / k$ , where $a$ is any characteristic dimension                          |
| $Pr$          | Prandtl number, $c_p \mu / k$  |
| $Q$           | Ratio of $q_{conv} / q_{cond}$   |
| $\bar{Q}$     | Heat transfer normalized by the conduction between concentric spheres                                |
| $q_{cond}$    | Heat transfer by conduction  |
| $q_{conv}$    | Heat transfer by convection  |

| <u>Symbol</u>    | <u>Description</u>   |
|------------------|--|
| $q_1$            | Heat transfer losses   |
| $q_{\text{rad}}$ | Heat transfer by radiation   |
| $r$              | Radial position  |
| $\bar{r}$        | Dimensionless radius defined by $\bar{r} = \frac{r - r(\theta)}{r_o(\theta) - r(\theta)}$                    |
| $Ra_a$           | Rayleigh number, $\rho^2 g \beta (T_i - T_o) a^3 c_p / \mu k$ , where $a$ is any characteristic of dimension |
| $Ra_a^*$         | Modified Rayleigh number, $Ra_a^* = Ra_a (L/R_i)$  |
| $r_{\text{av}}$  | Average radius, $(r_i + r_o)/2$  |
| $Rq$             | Ratio of characteristic dimensions   |
| $r_i, R_i$       | Inner body dimensions defined on page 38   |
| $r_o, R_o$       | Outer body dimensions defined on page 38   |
| $r(\theta)$      | Distance from the center of the inner body to the surface of the inner body                                  |
| $r_o(\theta)$    | Distance from the center of the outer body to the surface of the outer body                                  |
| $s$              | Half the length of the side of a cube  |
| $T$              | Local temperature  |
| $\bar{T}$        | Dimensionless temperature, $\bar{T} = \frac{T - T_o}{T_i - T_o}$   |
| $T_{\text{am}}$  | Arithmetic mean temperature $T_{\text{am}} = (T_i + T_o)/2$  |
| $T_f$            | Film temperature, $T_f = (T_o + T_i)/2$  |

| <u>Symbol</u> | <u>Description</u>   |
|---------------|--|
| $T_i$         | Inner body temperature   |
| $T_o$         | Outer body temperature   |
| $T_{vm}$      | Volume-weighted mean temperature defined for concentric spheres by equation (2.30) |
| $T_\infty$    | Temperature of the ambient, far from the inner body                                |
| $\Delta T$    | Temperature difference, $\Delta T = T_i - T_o$                                     |
| $x$           | Defined by equation A2.9   |
| $\bar{x}$     | Defined by $x/r_o$   |
| $\bar{y}$     | Defined by $y/r_o$   |
| $\bar{z}$     | Defined by $z/r_o$   |
| $\alpha$      | Defined by $r_i/r_o$ or $s/r_o$  |
| $\beta$       | Thermal expansion coefficient  |
| $\gamma$      | Over relaxation factor   |
| $\mu$         | Dynamic viscosity  |
| $\eta$        | Defined by equation A2.10  |
| $\pi$         | Ratio of circumference of circle to diameter, 3.14159                              |
| $\theta$      | Temperature probe location or angle in spherical coordinate system                 |
| $\rho$        | Density  |
| $\tau$        | Defined by equation (A2.8)   |
| $\phi$        | Angle in spherical coordinate system   |
| $\psi$        | Defined by equation (A2.11)  |

## CHAPTER I

### INTRODUCTION

The amount of work accomplished in the area of natural convection heat transfer within enclosures has increased over tenfold in the last twenty years. Despite the intensity of the effort, knowledge in this area is still limited. The demands for additional information in this area have also increased, as evidenced by the growing number of applications for natural convection heat transfer within enclosures. General areas of application include; nuclear design, electronic packaging, residential heating, and more recently in the solar energy field, solar collector design and utilization of natural circulation for energy storage systems.

The majority of the work accomplished in the area of natural convection heat transfer within enclosures has been experimental. The coupling and non-linearity of the governing equations and the fact that the boundary layer approximations are not valid for enclosures have forced experimental solutions. The relatively few analytical and numerical solutions available are generally limited in applicability.

The primary intent of this investigation is to experimentally determine the heat transfer and temperature distributions between isothermal (heated) inner bodies and their isothermal (cooled) cubical enclosure. The inner bodies used in conjunction with the cubical enclosure were spheres ( $0.45 \leq L/R_i \leq 1.89$ ), cylinders ( $0.66 \leq L/R_i \leq 1.47$ ), and cubes ( $0.64 \leq L/R_i \leq 1.62$ ). Four test fluids were utilized which



yielded Prandtl numbers ranging from 0.706 to 13847. These fluids were air ( $0.706 \leq Pr \leq 0.712$ ), water ( $4.50 \leq Pr \leq 10.20$ ), 20 cs ( $127.4 \leq Pr \leq 325.3$ ), and 96% aqueous glycerin ( $542 \leq Pr \leq 13847$ ). The 20 cs fluid refers to a Dow Corning 200 silicone fluid with a kinematic viscosity of 20 centistokes, measured at 25° Celsius. The glycerin represents a fluid whose properties are highly temperature dependent, as evidenced by the range of the Prandtl number.

The above mentioned experimental work will be compared with past investigations [15 - 18] which utilized basically the same inner bodies and fluids but with a spherical enclosure. An attempt will be made to determine the effects of different enclosures on the overall heat transfer. Of primary importance is the development of a general correlation equation to predict the heat transfer between arbitrarily shaped inner and outer bodies. The temperature profiles, while directly useful in themselves, can also provide experimental verification for any analytical or numerical solutions which may be advanced. The flow visualization data taken in this investigation will be used solely as an aid in interpreting the temperature profiles. No attempts will be made to categorize or characterize the flow patterns.

Empirical relations will be determined for each inner body and each test fluid. In addition, empirical equations will be found for the spherical and cubical enclosures. However, the major accomplishment would be the generalized correlation equation encompassing all of the

geometries and fluids. Such an equation could significantly increase the acceptability of the extrapolation of the test data to new cases - a significant contribution to the experimental investigation of natural convection heat transfer between bodies and their enclosures.

## CHAPTER II

### LITERATURE REVIEW

Natural convection processes are normally divided into two broad classifications. Flow in an extensive medium adjacent to a rigid body is termed external natural convection. Internal natural convection refers to flows within a fluid-filled cavity or flows bounded by surfaces. It should be noted now that the content of this chapter is not intended to be complete but is chosen for its usefulness to this particular investigation.

External flows have been extensively investigated experimentally, analytically, and numerically in the past. It has been found [33] that experimental data for the external problem may be correlated by

$$Nu_a = f(Gr_a, Pr) \quad (2.1)$$

where

$$Nu_a = \frac{\bar{h}a}{k} \quad (\text{Nusselt number}) \quad (2.2)$$

$$Gr_a = \frac{\beta \rho^2 a^3 \Delta T g}{\mu^2} \quad (\text{Grashof number}) \quad (2.3)$$

$$Pr = \frac{\mu c_p}{k} \quad (\text{Prandtl number}) \quad (2.4)$$

and  $a$  is some characteristic length dimension. For two and three dimensional bodies an additional dimensionless group is required to account for the geometry. The Grashof and Prandtl numbers are often combined into one dimensionless group, the Rayleigh number, which is

$$Ra_a = Pr \cdot Gr_a = \frac{c_p \beta \rho^2 a^3 \Delta T g}{k \mu} \quad (2.5)$$

In many cases it has been found that the Rayleigh number incorporates both the Grashof and Prandtl number effects, especially for Prandtl numbers outside the liquid metal range, so the correlation equations then take the form

$$Nu_a = f(Ra_a) \quad (2.6)$$

Geometric shapes such as vertical cylinders and rectangular blocks bear a close resemblance to the inner bodies used in this investigation. Holman [46] gives an expression for heat transfer (based on the data of Yuge) from isothermal spheres in air as

$$Nu_D = 2. + 0.43 Ra_D^{0.25} \quad \text{for } 1 \leq Ra_D \leq 10^5 \quad (2.7)$$

The fluid properties in this correlation and in subsequent correlations, unless otherwise noted, are evaluated at the film temperature,

$$T_f = \frac{T_\infty + T_i}{2} \quad (2.8)$$

for external natural convection or at the arithmetic mean temperature

$$T_{am} = \frac{T_i + T_o}{2} \quad (2.9)$$

for internal natural convection. A similar correlation obtained by Amato and Tien [3] for isothermal spheres in water is

$$Nu_D = 2. + 0.5(Ra_D)^{0.25} \quad \text{for } 3 \cdot 10^5 \leq Ra_D \leq 8 \cdot 10^8 \quad (2.10)$$

A correlation for natural convection heat transfer from isothermal vertical cylinders to a fluid of infinite extent is given by Holman [46] as

$$Nu_D = 0.59 Ra_D^{0.25} \quad \text{for } 10^4 < Ra_D < 10^9 \quad (2.11)$$

when

$$\frac{D}{\text{cylinder length}} > \frac{35}{Gr_{\text{cylinder length}}^{0.25}}$$

King [32] correlated data from several shapes including rectangular blocks. He found that the heat transfer could be correlated by

$$Nu_D = 0.60 Ra_D^{0.25} \quad \text{for } 10^4 < Ra_D < 10^9 \quad (2.12)$$

where

$$\frac{1}{D} = \frac{1}{\text{vertical dimension}} + \frac{1}{\text{horizontal dimension}}$$

More recently, Lienhard [34] noted that all of the laminar external natural convection problems, regardless of the shape of the immersed isothermal body, could be correlated by an equation of the form

$$Nu \approx 0.5 Ra^{0.25} \quad (2.13)$$

By equating the buoyant force on the body to the viscous drag force on the boundary layer, and by using velocity and temperature profiles for a vertical flat plate, Lienhard obtained the following result:

$$Nu_b = 0.52 Ra_b^{0.25} \quad (2.14)$$

where the characteristic dimension,  $b$ , is the distance travelled by the

boundary layer on the inner body. This equation is recommended by Leinhard for correlating laminar external natural convection heat transfer. Works by Ede [53] and Jacob [33] provide more complete summaries on external natural convection and the interested reader is referred to these sources.

Internal natural convection problems can be correlated in a manner similar to the external problems in the general form of equation (2.1), but additional ratios of physically meaningful characteristic dimensions of the system are required. For relatively simple geometries the correlating equations become

$$Nu_a = f(Gr_a, Pr, Rg) \quad (2.15)$$

where  $Rg$  is the ratio of the characteristic dimensions.

Natural convection within horizontal and vertical rectangular enclosures has been summarized by Weber [26], Ostrach [50], Jacob [33], and others and will not be discussed further. A summary of natural convection within concentric cylindrical and spherical annuli is also given by Weber [26]. Some of this material will be repeated here for completeness and easy reference. The rest of this discussion of internal convection is divided into six parts. These are concentric cylinders, concentric spheres, eccentric spheres, cylinder-sphere geometry, cube-sphere geometry, and temperature profiles.

#### CONCENTRIC CYLINDERS

To correlate the heat transfer between concentric cylinders

Beckman [33], Kraussold [33], Liu et al [11], and Lis [12] all defined a new dependent correlation parameter,  $k_{\text{eff}}/k$  or  $q_{\text{conv}}/q_{\text{cond}}$ , which is a modified Nusselt number and includes the effects of convection relative to the heat which would be transferred by pure conduction. The correlation equation (2.15) is then written as

$$\frac{q_{\text{conv}}}{q_{\text{cond}}} = \frac{k_{\text{eff}}}{k} = f(\text{Gr}_a, \text{Pr}_a, \text{Rg}). \quad (2.16)$$

Physically  $k_{\text{eff}}$  is the thermal conductivity a motionless fluid must have to transmit the same amount of energy as the moving fluid. The ratio  $k_{\text{eff}}/k$  has a lower limit of unity when the convective activity becomes negligible.

For concentric cylinders the ratio is equivalent to

$$\frac{q_{\text{conv}}}{q_{\text{cond}}} = \frac{k_{\text{eff}}}{k} = \frac{q_{\text{conv}} \ln(D_o/D_i)}{2 k(T_i - T_o)} \quad (2.17)$$

Beckman [33] investigated this configuration in 1931 for air, hydrogen, and carbon dioxide for diameter ratios,  $D_o/D_i$ , from 1.2 to 8.1 and values of  $\text{Gr}_{D_i}$  from  $10^3$  to  $10^7$ . A critique by Liu et al [11] points out that limited data and inconsistent results at the higher diameter ratios would limit the accurate application of Beckman's model to diameter ratios with an upper limit of 2.1. Also Beckman's failure to insulate the ends of his test apparatus led to considerable axial conduction

errors.

Kraussold [33] extended Beckmann's work by using water and oil to account for the Prandtl number effect. For a Prandtl number between 7 and 4000 and diameter ratios from 1.2 to 3.0 Kraussold determined the following expressions for  $k_{eff}/k$ :

$$k_{eff}/k = 1.0 \text{ for } Ra_L < 10^3 \quad (2.18)$$

$$k_{eff}/k = 0.11 Ra_L^{0.29} \text{ for } 6.4 \cdot 10^3 < Ra_L < 10^6 \quad (2.19)$$

$$k_{eff}/k = 0.40 Ra_L^{0.20} \text{ for } Ra_L > 10^6 \quad (2.20)$$

where  $L = \frac{D_o - D_i}{2}$ .

Liu et al [11] proposed the following empirical correlations for the heat transfer between concentric cylinders:

$$\frac{k_{eff}}{k} = 1.0 \text{ for } A < 10^3 \quad (2.21)$$

$$\frac{k_{eff}}{k} = 0.135 (A)^{0.278} \text{ for } 3.2 \cdot 10^3 < A < 10^8$$

$$\text{and } 0.25 \frac{L}{D_i} < 3.25 \quad (2.22)$$

where  $A = \frac{Pr^2 Gr_L}{1.36 + Pr}$  and  $0.7 < Pr < 3672$ .

Lis [12] correlated  $k_{eff}/k$  for Rayleigh numbers,  $Ra_{D_i}$ , between  $4 \cdot 10^4$  and  $4.7 \cdot 10^{10}$ , diameter ratios  $D_o/D_i$  between 2.0 and 4.0, and Prandtl numbers between 0.645 and 1.32. His empirical correlation is:



$$\log\left(\frac{k_{\text{eff}}}{k}\right) = 0.0794 + 0.0625 \log X + 0.0154 (\log X)^2 \quad (2.23)$$

where

$$X = Ra_{D_i} \cdot (1 - D_i/D_o)^{6.5}.$$

Grigull and Hauf [13] used a Mach-Zehnder interferometer to make their measurements with air as the test fluid. Bishop [26] determined a correlation for  $k_{\text{eff}}/k$  from Grigull and Hauf's data which was

$$\frac{k_{\text{eff}}}{k} = 0.163 Gr_L^{0.2578} \quad \text{for } 5 \cdot 10^3 < Gr_L < 7.16 \cdot 10^5$$

and  $0.32 < L/D_i < 2.65$ . (2.24)

Itoh et al [2] have correlated the data given by Beckman, Kraussold, and Grigull and Hauf by defining the Grashof number as

$$Gr_m = \frac{\rho^2 g \beta (T_i - T_o) [r_m \ln(r_o/r_i)]^3}{\mu^2} \quad (2.25)$$

where  $r_m = \sqrt{r_i r_o}$ .

This correlation is

$$\frac{q_{\text{conv}}}{q_{\text{cond}}} = 0.20 (Pr Gr_m)^{0.25} \quad (2.26)$$

for  $7.1 \cdot 10^3 < (Pr Gr_m) < 10^8$ .

This correlation seemed to fit the data well although no error analysis was presented.

More recently Raithby and Hollands [7] have presented a method for

correlating both external and internal natural convection. By balancing viscous and buoyancy forces near the wall (similar to Lienhard's [34] simplified analysis) they were able to obtain an approximate expression for the conduction thickness. This then enabled them to calculate the heat transfer, or in the more complicated internal natural convection problems, they found new correlation equations. For concentric cylinders the equation developed by them is

$$\frac{q_{\text{conv}}}{q_{\text{cond}}} = \frac{C \ln(D_o/D_i)}{2 L^{0.75} (D_i^{-0.6} + D_o^{-0.6})^{1.25}} \quad (2.27)$$

where C (obtained by correlating the data of Beckman, Grigull and Hauf, Kraussold, and Liu, Mueller, and Landis) was equal to 0.634. Most of the data were within  $\pm 10\%$  of the equation except for the data of Liu et al [11] which displayed considerable scatter. Curvature effects become important when  $L/D_i < 0.3$ , and a trial and error procedure must be used to calculate the heat transfer.

In addition to the experimental results, analytical and numerical results have been obtained over limited ranges of the Prandtl and Rayleigh numbers. The interested reader is referred to the literature [9, 24, 44].

#### CONCENTRIC SPHERES

Bishop et al [16] first correlated the expression  $q_{\text{conv}}/q_{\text{cond}}$  for

isothermal concentric spheres. With air as the test fluid and for diameter ratios ranging from 1.19 to 3.14 (or  $0.25 < L/r_i < 1.5$ ) they obtained the empirical correlation

$$\frac{q_{\text{conv}}}{q_{\text{cond}}} = 0.106 \text{ Gr}_L^{0.276} \text{ for } 2 \cdot 10^4 < \text{Gr}_L < 3.6 \cdot 10^6 \quad (2.28)$$

where

$$\frac{q_{\text{conv}}}{q_{\text{cond}}} = \frac{q_{\text{conv}} L}{4\pi k \Delta T r_i r_o} \quad (2.29)$$

The fluid properties in this correlation were evaluated at a volume-weighted mean temperature defined as

$$T_{\text{vm}} = \frac{(r_{\text{av}}^3 - r_i^3) T_i + (r_o^3 - r_{\text{av}}^3) T_o}{r_o^3 - r_i^3} \quad (2.30)$$

where each fluid particle within the gap is arbitrarily assigned the temperature of the nearer surface. Equation (2.29) fit the data with maximum deviations of -13.4 per cent and +15.5 per cent.

Scanlan et al [15] extended this work to account for a Prandtl number effect. Taking data with water and two silicone oils they obtained Prandtl numbers in the range of 4.7 to 4148. The overall correlation, which included the air data, was given by

$$\frac{q_{\text{conv}}}{q_{\text{cond}}} = 0.202 \text{ Ra}_L^{0.228} \left(\frac{L}{r_i}\right)^{0.252} \text{ Pr}^{0.029} \quad (2.31)$$

with an average deviation of 13.7 percent. A simpler correlation resulted in

$$\frac{q_{\text{conv}}}{q_{\text{cond}}} = 0.228 (Ra_L^*)^{0.226} \quad (2.32)$$

where

$$Ra_L^* = Ra_L \left( \frac{L}{r_i} \right) \quad (2.33)$$

This equation resulted in an average deviation of 15.6 percent. Fluid properties in both equations were evaluated using  $T_{vm}$ .

Raithby and Hollands [7] correlated the data of Bishop et al [16] and Scanlan et al [15]. Their equation took the form

$$\frac{q_{\text{conv}}}{q_{\text{cond}}} = \frac{0.61 L^{0.25} Ra_L^{0.25}}{D_o D_i (D_i^{-1.4} + D_o^{-1.4})^{1.25}} \quad (2.34)$$

where the constant 0.61 was found from the experimental data. Except for the water data their correlation seems to fit the data slightly better than equation (2.32). Mack and Hardee [39] obtained an analytical solution for this geometry which was restricted to low Rayleigh numbers.

#### ECCENTRIC SPHERES

Weber et al [18] considered natural convection from a vertically eccentric sphere to a cooler enclosing sphere. By using a conformal mapping technique to map the eccentric spheres to concentric spheres they were able to correlate all of the eccentric sphere data using equation (2.32). An error analysis indicated that the eccentric data were represented by the equation to within an average deviation of 18.2 per cent. These data included Prandtl numbers from 4.7 to 4148, Rayleigh

numbers based on gap width from  $4 \cdot 10^2$  to  $9 \cdot 10^7$ , and eccentricities between  $-0.75 \leq e/(r_o - r_i) \leq +0.75$ . The mapping technique did account for the minor effect (to increase the heat transfer rate) of the eccentricity.

Raithby and Hollands [7] noted that the eccentricity should not affect their model until the conduction layers on the inner and outer surfaces touch. Using equation (2.34) they were able to correlate most of the eccentric sphere data to within  $\pm 10$  percent of their equation. For an eccentricity,  $e/(r_o - r_i) = -0.75$  (down), their equation was 10% too low. This would be expected since an eccentricity of  $-0.75$  should have the greatest effect on the heat transfer.

#### CYLINDER-SPHERE

McCoy et al [17] obtained test results for the heat transfer between isothermal, vertical cylinders with hemispherical ends and their isothermal spherical enclosure. Using  $T_{vm}$  to evaluate the fluid properties they found that equation (2.32) could also be used to correlate the vertical cylinder data if the gap,  $L$ , is defined as the hypothetical gap width between the outer sphere and an inner sphere of volume equal to that of the cylindrical inner body. Their data fit equation (2.32) with an average deviation of 13.8 per cent. The conduction factor in  $q_{conv}/q_{cond}$  had to be evaluated numerically for this geometry.

#### CUBE-SPHERE

McCoy [27] investigated the heat transfer from an isothermal cubical inner body to an isothermal enclosing sphere. An overall

correlation equation was obtained in the form

$$Nu_L \frac{r_i}{r_o} = 0.130 (Ra_L)^{0.253} \quad (2.35)$$

where

$$r_i = \frac{\text{cube length}}{2} \quad \text{and} \quad L = r_o - r_i .$$

This equation fit the data with an average deviation of 6.2 per cent for  $0.71 < Pr \leq 3969$ ,  $4.8 \cdot 10^5 < Ra_L < 3.4 \cdot 10^8$ , and  $0.988 < (L/r_i) < 2.908$ .

### TEMPERATURE PROFILES

Temperature profile and flow visualization results are available for the enclosure geometries discussed above [10-18, 20, 25-27, 30, 45, 52]. In addition, flow visualization results are available for heat transfer between an isothermal sphere and an isothermal enclosing cube [19, 28, 29]. Some of the general trends in the temperature profile results are discussed below.

It has been found [15-18] that the temperature profiles (when plotted in terms of dimensionless radius and temperature ratios) for all the geometries could be divided into five regions: 1) a steep drop next to the inner body, 2) a gently curved inner transition region, 3) a region of small temperature gradient, 4) a gently curved outer transition region, and 5) a steep drop next to the outer body. The large temperature gradients next to the inner and outer bodies are due to the high rate of radial heat transfer attributed to the large velocities next to the bodies. The transition regions connect the steep drop regions with

the flat profile region of low velocity.

It was also noted by these same investigators that the form of the temperature profile at a given angular position was independent of the temperature difference as long as the Prandtl number remained relatively constant. The effect of increasing the Prandtl number for concentric spheres was to increase the radial extent of the transition regions due to the thickening of the boundary layers. For the cylinder-sphere geometry an increase in the Prandtl number generally gave a higher value of the dimensionless temperature ratio. The lower gap region was postulated to be more stagnant with the lower Prandtl number fluids. In the upper region the flow separated from the inner surface near the junction of the cylinder and its hemispherical end. Confirmation of this was made by Powe et al [52] in a flow visualization study for this geometry.

For the smaller values of  $r_o/r_i$  it was found [15-18] that the profiles were ordered differently. It was postulated that a multicellular flow pattern existed in the upper gap region. This was later confirmed with flow visualization data [20, 52].

Weber et al [18] for eccentric spheres found that a negative eccentricity enhanced the convective motion, while a positive eccentricity promoted flow stabilization. This was confirmed by Powe et al [52] in a flow visualization study.

In all the enclosure configurations mentioned above, temperature

inversions were noted for some combination of fluid, diameter ratio, and temperature difference. These temperature inversions were attributed to the high rate of angular convection of energy relative to the radial transport.

The temperature profiles and flow visualization data showed that another trait common to all the enclosure geometries discussed was the invariance of the overall heat transfer with the type of flow pattern existing within the gap. Even the steadiness or unsteadiness of the flow had negligible affect on the overall heat transfer.

Powe [ 5 ] looked at the range of relative gap widths ( $L/r_i$ ) for which the empirical correlations for concentric spheres and cylinders are applicable. The upper bound for the heat transfer in the enclosures is that value predicted by the infinite atmosphere solution. The lower limit is taken as that value of the Nusselt number given by pure conduction. Minimum and maximum values of  $L/r_i$  for the enclosure equations are presented as a function of  $Ra_D$ . Limits on  $L/r_i$  for these (and other) empirical equations for natural convection in enclosures should be considered.

The amount of data on natural convection in enclosures has increased greatly in the past few years. However, understanding of this area is far from complete. This current study utilizes concentric spherical, cylindrical, and cubical inner bodies with an isothermal enclosing cube to determine the effect, if any, of a different enclosing



geometry. The preceding discussion has pointed out the need for a consistent means of correlating enclosure data and has shown three possible approaches to the problem. If the effect of changing the outer geometry is small then possibly Lienhard's [34] boundary layer length parameter for external natural convection could be used for the enclosure problem. The work of Raithby and Hollands [7] provides a physically meaningful method for correlating both external and internal natural convection heat transfer. Its use is limited by three factors: 1) it is limited to configurations where the inner and outer conduction layers do not touch, 2) with smaller inner bodies the curvature effects become important and the heat transfer must be found by trial and error, and 3) the method cannot handle more complicated inner body shapes such as the cube. It should be noted that their method did show the minor effect of the type of flow pattern on the overall heat transfer rate. In addition their model is unable to predict any change in the overall heat transfer with change in outer geometry. A third approach is the use of a correlation similar to equation (2.32). Although there is no physical reasoning behind the use of  $q_{\text{conv}}/q_{\text{cond}}$ , it does seem reasonable to use this ratio since  $q_{\text{cond}}$  is a strong function of the geometry. This procedure has worked in the past and seems to be the best hope to correlate the more complicated geometries such as the cube-cube configuration.

## CHAPTER III

### EXPERIMENTAL APPARATUS AND PROCEDURE

#### EXPERIMENTAL APPARATUS

The data in this investigation were obtained from three different experimental apparatus. A 10.5 inch (length of a side) cubical test space and a 9.828 inch (diameter) spherical test space were used in combination with different size spherical, cylindrical, and cubical inner bodies to acquire the heat transfer and temperature profile data. A detailed description of the apparatus employing the spherical test space is given by Weber [26] and McCoy [27]. The flow visualization data were obtained using the apparatus described by Eyler [29] and Larson [28] with the cubical test space enlarged to 10.0 inches on a side. The heat transfer apparatus employing the cubical test space, Figure 3.1, was used for taking most of the heat transfer data and is described in detail below.

A schematic of the apparatus, Figure 3.2, shows the cubical water jacket, which measured 15.0 inches on a side. The water jacket consisted of six separate rectangular channels 1.25 inches in width. Several inlet and outlet ports on each of the channels, fed by a manifold system, ensured a uniform flow over each of the sides. The flow rate of cooling water to each of the channels could be independently adjusted, to ensure that the cube enclosing the test space was isothermal. The cooling water was circulated by a closed system consisting of a chiller, pump, and reservoir (far left in Figure 3.1). Both the enclosing cube































































































































































































































































































































































































































